



# LUND UNIVERSITY

## Spatially Resolved Temperature Measurements Above a Burning Wood Pellet Using Diode Laser-Based Two-Line Atomic Fluorescence

Borggren, Jesper; Weng, Wubin; Aldén, Marcus; Li, Zongshan

*Published in:*  
Applied Spectroscopy

*DOI:*  
[10.1177/0003702817746996](https://doi.org/10.1177/0003702817746996)

2018

[Link to publication](#)

*Citation for published version (APA):*  
Borggren, J., Weng, W., Aldén, M., & Li, Z. (2018). Spatially Resolved Temperature Measurements Above a Burning Wood Pellet Using Diode Laser-Based Two-Line Atomic Fluorescence. *Applied Spectroscopy*, 72(6), 964-970. <https://doi.org/10.1177/0003702817746996>

*Total number of authors:*  
4

*Creative Commons License:*  
CC BY

### General rights

Unless other specific re-use rights are stated the following general rights apply:  
Copyright and moral rights for the publications made accessible in the public portal are retained by the authors and/or other copyright owners and it is a condition of accessing publications that users recognise and abide by the legal requirements associated with these rights.

- Users may download and print one copy of any publication from the public portal for the purpose of private study or research.
- You may not further distribute the material or use it for any profit-making activity or commercial gain
- You may freely distribute the URL identifying the publication in the public portal

Read more about Creative commons licenses: <https://creativecommons.org/licenses/>

### Take down policy

If you believe that this document breaches copyright please contact us providing details, and we will remove access to the work immediately and investigate your claim.

LUND UNIVERSITY

PO Box 117  
221 00 Lund  
+46 46-222 00 00



**Title page:**

## **Spatially resolved temperature measurements above a burning wood pellet using diode laser-based two-line atomic fluorescence**

*J. Borggren, W. Weng, M. Aldén and Z.S. Li*

*Division of Combustion Physics, Lund University*

This is the peer reviewed version of the following article: [J. Borggren, W. Weng, M. Aldén and Z.S. Li, ‘*Spatially resolved temperature measurements above a burning wood pellet using diode laser-based two-line atomic fluorescence*’, **Applied Spectroscopy** **72**, 946-970 (2018).], which has been published in final form at: <http://DOI: 10.1177/0003702817746996>

# Spatially resolved temperature measurements above a burning wood pellet using diode laser-based two-line atomic fluorescence

*J. Borggren, W. Weng, M. Aldén and Z.S. Li*

*Division of Combustion Physics, Lund University*

## ***Abstract***

Diode laser-based two-line atomic fluorescence (TLAF) thermometry applied to flames of combusting wood pellets is demonstrated. The pellets are placed in the hot product gas ( $O_2$  concentration 1.7%) of gallium seeded laminar flames stabilized on a multi-jet burner. The calibration-free technique provides one dimensional spatial temperatures with sufficient temporal resolution to resolve all combustion stages of a pellet even in highly sooting flames. The temperature above a burning pellet was found to decrease due to the release of volatile gases and the accuracy and precision of the technique is assessed at flame temperatures.

**Keywords:** Two-line atomic fluorescence, thermometry, diode lasers, biomass combustion

## ***Introduction***

The evermore stringent regulations to reduce the environmental impact of emissions from heat and energy production in today's society are increasing the demand for fossil-free and renewable energy sources. A renewable energy source gaining more attention as a replacement for fossil fuels is biomass [1, 2], and especially in coal fired power plants where co-firing biomass is being increasingly used to meet emission regulations [3-5]. Biomass is an organic source of energy that, compared to fossil fuels, has the main advantage of being  $CO_2$  neutral and thereby considerably reducing the environmental impact [6]. Biomass does, however, generally suffer from low bulk densities which can be overcome with various methods, e.g. pelletisation, where the biomass is compressed to increase the energy density and the homogeneity of the raw material of the fuel [7].

The increasing demand of biomass for combustion and gasification has surged an interest from the research community striving to understand and model the process of combustion accurately [8-10]. The combustion of biomass is a complex process involving many phases, e.g. de-volatilization, char oxidation and ash cooking. Additional complications occur due to differences between biomass sources used, such as different wood types, straws or other organic substances. A necessity for the development of new and accurate models is in-situ experimental measurements of parameters such as species concentrations, flow fields and temperatures for model validation [8, 11, 12]. Experimental measurements using optical techniques can provide in-situ and non-intrusive measurements with the required spatial and temporal resolution. However, the combustion of pellets produces a difficult operating environment for optical techniques due to the release of particulates and soot. Hence, optical measurements in biomass applications are scarcely found in the literature.

Temperature, being one of the governing physical properties in a combustion process due to its strong relation to the chemical reaction rate, is of great importance for understanding the combustion process. Temperature measurements above burning pellets using both thermocouples and optical technique have previously been demonstrated to provide useful data [13, 14]. Thermocouples do, however, suffer from being intrusive, limited to point measurements and have a slow time response. An optical technique successfully implemented for temperature measurements above pellets, in a reactor with good accuracy and temporal resolution, is calibration-free wavelength modulation spectroscopy (CF-WMS) [14]. CF-WMS is a line-of-sight (LOS) technique providing path-integrated

temperatures along the laser beam which could be advantageous in systems with limited optical access; however, spatial information is lost and the applicability of the technique in environments with temperature gradients is diminished. A promising optical technique able to provide spatially and temporally resolved temperature measurements in harsh environments is two-line atomic fluorescence (TLAF) [15, 16].

In TLAF an atomic species with suitable electronic transitions, such as of a three-level lambda system is seeded to the flame. The group III metals, e.g. indium, gallium and thallium, have been shown to be suitable for temperature measurements [16-18]. The two lower lying electronic levels are excited to the common upper state and the resulting fluorescence signals, being separated in time, are recorded. The strength of the fluorescence signal is proportional to the population of each state which in turn is governed by the temperature dependent Boltzmann distribution. Temperature information can be derived from the ratio of the intensity of the two fluorescence signals. TLAF offers beneficial features such as insensitivity to elastic scattering, being independent on the gas composition and strong fluorescence signals from atoms [19]. However, an atomic species normally not present in the combustion environment needs to be seeded.

TLAF using diode lasers have been demonstrated to have capabilities for temperature measurements in both low pressure [20, 21] and atmospheric flames [22]. Previous work using diode lasers have, however, all used a detection scheme that is sensitive to elastic scattering and thus not suitable in heavily sooty flames, although there have been successful applications in low-sooting flames [20]. In the elastic detection scheme the fluorescence signal of only one transition is detected, independent on excitation wavelength, providing the benefit of not having to calibrate for the difference in detector efficiencies at different wavelengths and also allowing for a single detector to be used. In the other possible detection scheme the non-resonant fluorescence is detected for each excitation requiring a detector calibration.

In this work, the two detection schemes of diode-laser based TLAF is combined for temperature measurements in particle laden and heavily sooting flames without the need for calibration from a second thermometric technique. The technique is especially applicable for measurements of the relatively slow transient temperature behaviour of a burning pellet in a hot flow. The accuracy and precision of the technique is evaluated and the technique is applied to measurements of burning wood pellets.

## ***Experimental Setup***

TLAF requires a temperature marker in the form of an atomic species, probeable by laser excitation, to be seeded into the flame. The electronic configuration of the atomic states should be that of a three-level lambda system where the energy splitting between the two lower lying states determines the temperature range in which the atom is suitable. The energy splitting is inversely proportional to the temperature precision and at the same time the signal strength of the upper state decreases with a higher energy splitting there is thus a trade-off between the signal-to-noise and precision. Indium and gallium have both been used for temperature measurements in flames previously [18, 23]. In this work gallium was chosen as the seeded species because it has a better sensitivity at lower temperatures that could be expected in biomass combustion. The seeding system described in [24] was used to seed the flame with tri-methyl-gallium (TMGa) molecules that upon passage through the reaction zone dissociates into free gallium atoms that can be excited with a laser. An inert gas, such as nitrogen, is flowed through a bubbler filled with TMGa, where the TMGa will undergo sublimation due to the high vapour pressure and saturate the gas that carries the organometallic substance to the burner

where it is mixed with the premixed fuel and air mixture. The flow through the bubbler and the bubbler temperature determines the concentration of gallium in the flame. For the present experiment the temperature of the bubbler was set to  $-15^{\circ}\text{C}$  and the carrier gas flow to 0.1 l/min which from previous experiments results in ppb levels of gallium atoms in the product zone [18].

A schematic of the optical setup is shown in Figure 1. The gallium atoms were probed with two external cavity diode lasers (ECDL) (Toptica DL100PRO) with wavelengths 403.3 nm and 417.2 nm, and with reported linewidths of  $<1$  MHz. The laser power was  $\sim 5$  mW in the interrogation region and the beam diameter of approximately 1 mm. The two laser beams were overlapped with a dichroic mirror and directed through the burner 10 mm above the pellet. Before the burner, the overlapped beams were split with a wedged glass plate, where one reflection was sent to a photodiode, to monitor the power, and the second reflection to a wavemeter (HighFinesse UV6-200) to monitor the wavelength. The photodiode was calibrated using a power meter (Thorlabs S302C) to allow for measurement of laser power for the two lasers during a measurement. After the burner part of the beam was sent to a second photodiode to measure the absorption and part of the beam was sent to a Fabry-Perot interferometer to ensure the lasers were running single-mode. An intensified CCD camera (PIMAX2), aligned perpendicular to the propagation direction of the laser beam, acquired images of the laser-induced fluorescence (LIF) signal. The camera was mounted with a stereoscope orientated to produce two separate images on the camera chip, see Figure 1. Filters for the two possible fluorescence wavelengths,  $\lambda=403$  nm and  $\lambda=417$  nm, with a filter FWHM of  $\pm 5$  nm and peak transmission of 70% were mounted in the stereoscope. The two separate images were overlapped using the generic built-in image transformation function in MatLab. The LIF signal was integrated vertically to provide spatially resolved temperature measurements in one dimension along the beam, both to increase the signal-to-noise ratio and avoid errors from laser profile compensation.

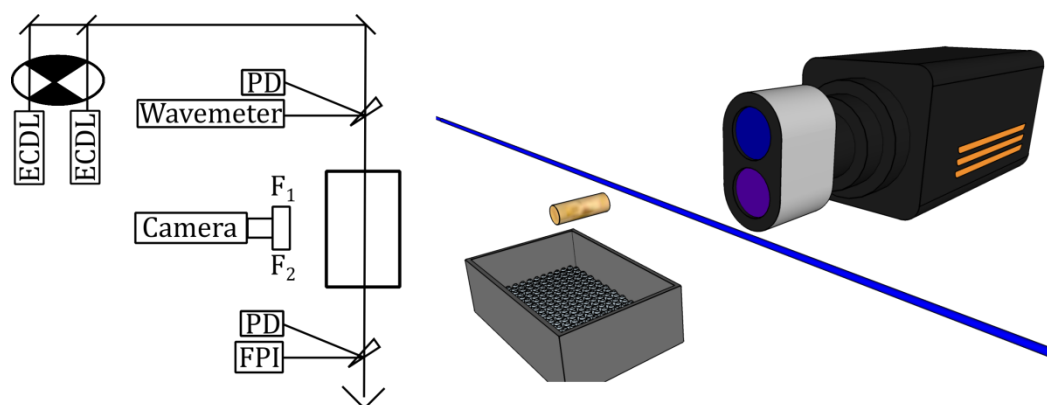


**Figure 1** Schematic of the experimental to the left. The camera is mounted with a stereoscope with filters for the two fluorescence wavelengths. *PD* – Photodiode, *ECDL* – External cavity diode laser, *FPI* – Fabry-Perot interferometer, *F1* and *F2* – filters. To the right is a 3D visualization of the optical alignment of the laser in regards to the pellet, burner and camera.

For each temperature measurement three individual frames were acquired by the camera, one for the background and one for each laser excitation. A chopper synchronized to the camera was used to switch between the three acquisition cases. For the background measurement both lasers are blocked simultaneously by the chopper. With the rotation of the chopper the lasers will sequentially excite the atoms in the flame while the other laser is blocked. Hence, one image is acquired for each exciting laser. This acquisition method allows for compensation of both slow fluctuations in the measurement region and changes in the seeding concentrations prevalent in the combustion process of burning pellets. For the present experiments the time resolution was limited to the acquisition speed of the camera which was at most 9 Hz resulting in a temporal resolution of 0.33 s for a single temperature

measurements. Hence, an exposure time in the order of milliseconds can be used without decreasing the temporal resolution. For the measurements presented in this work the exposure time was set to 3 ms.

The probed transitions of gallium are  $4^2P_{1/2} \rightarrow 5^2S_{1/2}$  at 403.3 nm and  $4^2P_{3/2} \rightarrow 5^2S_{1/2}$  at 417.2 nm and the detection configuration results in a total of four detected fluorescence signals, a resonant and a non-resonant fluorescence signal for each excited transition. The fluorescence signal can be denominated as  $F_y^x$  where the superscript is the excitation transition and subscript the fluorescence transition, e.g.  $F_{21}^{02}$  is the fluorescence signal acquired upon excitation of the lowest ground state (level 0) to common upper state (level 2) while detecting the non-resonant fluorescence to the upper ground state (level 1). Three fluorescence ratios of interest can be constructed from these signals; two ratios are constructed from the fluorescence signals detected for the same filter ( $R_{21} = F_{21}^{12}/F_{21}^{02}$  and  $R_{20} = F_{20}^{12}/F_{20}^{02}$ ) and one ratio ( $R_{nr} = F_{20}^{12}/F_{21}^{02}$ ) for the non-resonantly detected fluorescence signals. The resonant ratios are only possible to measure in flames without any elastic scattering. They need, however, only be measured once to calibrate the system. The non-resonant ratio  $R_{nr}$  has to be compensated with a calibration factor due to differences in the quantum yield for the detector at the two different wavelengths and the difference in collection efficiency. The calibration factor is the ratio between the derived mean temperature for  $R_{21}$  and  $R_{20}$  and the uncalibrated temperature of  $R_{nr}$ .

The temperature is calculated by comparing the experimental fluorescence ratio  $R$  to a simulated ratio  $R_{sim}$ . The simulated ratio is a function of the overlap between the laser and absorption profile  $g$ , the Boltzmann distribution  $f$  and the Einstein coefficient for stimulated absorption  $B$ .

$$R_{sim}(T) = \frac{g_{12}(\lambda_{12}, T) \cdot f_1(T) \cdot B_{12}}{g_{02}(\lambda_{02}, T) \cdot f_0(T) \cdot B_{02}}$$

The overlap function,  $g$ , can be determined from an excitation scan while simultaneously recording the wavelength on the wavemeter. Excitation scans of the two transitions are presented in Figure 2 together with a least-square fit using the information presented in Table 1 and with the fitting parameters amplitude, temperature, and background.

**Table 1** Information used for simulating the hyperfine structure. The values for the hyperfine structure are from [25] and the relative intensities are calculated from the Clebsch-Gordan coefficients.

Transition	Wavelength [nm]	Einstein A coefficient [ $10^8 \text{ s}^{-1}$ ]	Hyperfine splittings [GHz]	Relative intensities
<b>Ga</b> $4^2P_{1/2} \rightarrow 5^2S_{1/2}$	403.3	0.485	0	1.0000
			2.138	1.0000
			2.678	0.2000
			4.816	1.0000
<b>Ga</b> $4^2P_{3/2} \rightarrow 5^2S_{1/2}$	417.2	0.945	0	0.3571
			0.319	0.3571
			0.447	0.1429
			2.138	1.0000
			2.457	0.3571
			2.585	0.0714

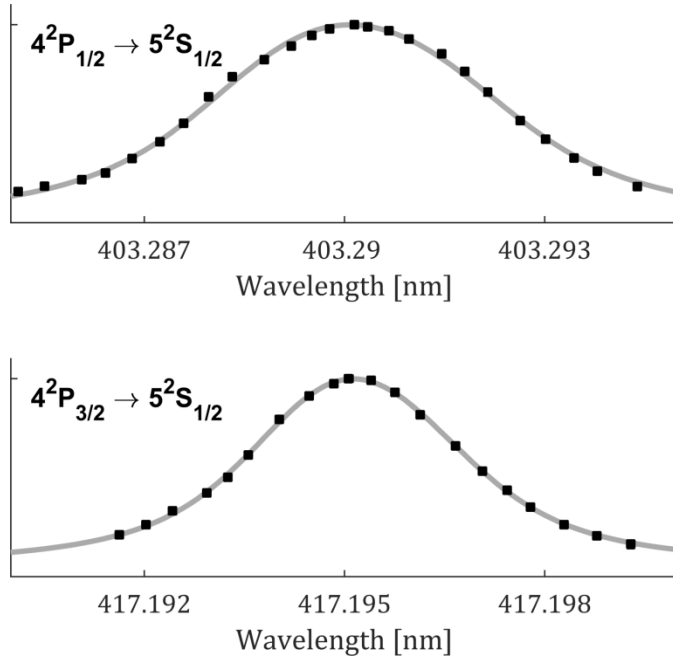


**Figure 2** Excitation scans of the two probed transitions of gallium (black squares) performed in the burner with equivalence ratio 1.0 and the corresponding best fit as the grey line. The wavelength is recorded on a wavemeter and the intensity is acquired on the camera. The lasers are tuned to the peak of the absorption profile during the temperature measurements.

A multi-jet burner, described in detail in [26], was employed for both the temperature calibration and for the burning of the pellets. The burner consists of 181 small jet-flames enclosed in an area of 60x100 mm by two shield rings resulting in an outlet 35 mm above the jets. A stabilizer with the same dimensions as the burner was located 30 mm above the outlet. The gas composition of the laminar jet flames was a mixture of methane, nitrogen and oxygen with total flow of 22 l/min with the proportions of  $O_2:N_2$  being 1:2.5. A nitrogen co-flow of 11 l/min were used for all equivalence ratios.

## Results

For the calibration measurements the laser beam was aligned to a height of 7 mm above the burner outlet and the equivalence ratio was varied between 0.8 and 1.3 to allow for comparison to previously measured temperatures in the same burner with coherent anti-Stokes Raman spectroscopy [18]. The calibration temperatures derived from the mean of the resonant ratios  $R_{21}$  and  $R_{20}$  are presented as the red squares in Figure 3. These temperatures agree well with previous TLAf and CARS measurements indicating that the use of a stereoscope does not affect the measurements. The uncalibrated non-resonant temperature measurements derived from  $R_{nr}$ , shown as the black circles in Figure 3, are observed to be of a constant lower temperature than the resonant temperature measurements. The mean calibration factor is calculated to be  $CF = \frac{T(R_{21}) + T(R_{20})}{2 T(R_{nr})} = 1.0293 \pm 0.0035$ . Multiplying the temperature from the non-resonant fluorescence ratio  $T(R_{nr})$  with the calibration factor yields the calibrated non-resonant temperatures, presented as the grey triangles in Figure 3. As mentioned previously, the seeding concentration was kept low enough as to avoid radiation trapping.



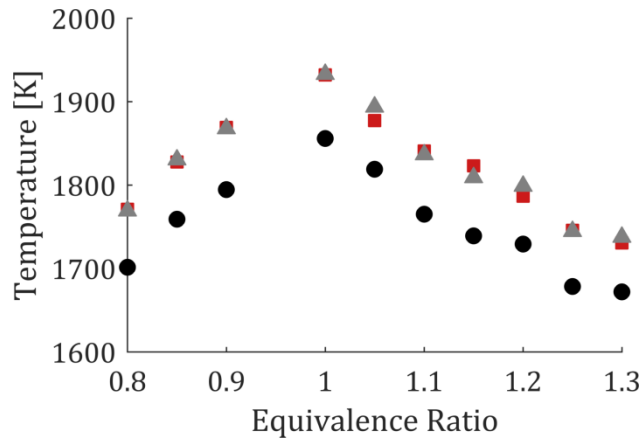


**Figure 3** A temperature calibration was conducted at equivalence ratios between 0.8 and 1.3. *Red squares* - average temperature from the resonant measurement, *black circles* – uncompensated non-resonant TLAF and *grey triangles* - compensated non-resonant TLAF.

The temperature of a combusting wood pellet in a hot oxidizing atmosphere was investigated by placing a pellet on two thin ceramic rods just above the burner outlet in the centre of the burner and the laser beam was aligned to pass 10 mm above the top of the pellet. The equivalence ratio of the flame was set to 0.9 to have a low abundance of oxygen resulting in a concentration of 1.7% in the product gases. The pellets were made of pine wood and were cylindrical in shape with a diameter of 4 mm and a length of 10 mm.

At the start of a measurement the pellet was inserted into the hot product gases and all combustion stages of the pellet was recorded. Photographs of the different combustion stages taken with a system camera are shown in Figure 4. In all frames a blue line of the laser-induced fluorescence of gallium is seen in the middle of the image. The fluorescence is seen to be weaker above the wood pellet due to changes in the flow field as well as due to the release of volatile gases from the pellet. The photographs are numbered in sequential order and the first frame shows the LIF just before insertion of the pellet. Early flaming is seen in photographs 2 and 3 and late flaming is observed in photograph 4. A strong elastic scattering is present in this flaming stage due to the generation of soot. The after-flame stage is seen in photograph 5 and the last stage is the smouldering and final glowing in photograph 6.

A strong LIF signal was observed in the reaction zone of the diffusion flame from the burning volatile gases due to the increase in local mixture fraction which is consistent with other measurement where a strong signal dependence on the equivalence ratio have been shown [27]. The combination of the strong signal in the reaction and the much weaker signal above the pellet demands a large dynamic range of the camera. Due to the limited dynamic range of the camera and to the need to avoid saturation of the detector a signal-to-noise ratio (SNR) of 6:1 was acquired for each laser above the pellet. The SNR was calculated as the mean intensity divided by the pixel-to-pixel noise in the region of interest. Before insertion of the pellet, corresponding to photograph 1, the SNR was determined to be 25:1.

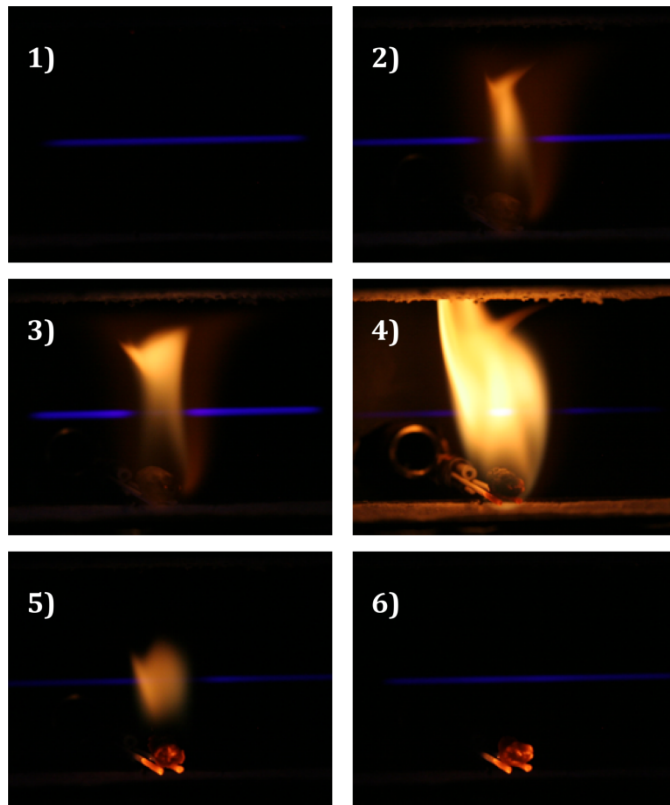


**Figure 4** Photographs of different stages in the combustion process of a wood pellet numbered in sequential order. The blue line is the laser-induced fluorescence signal of gallium in the flame. Some elastic scattering can be seen in frame 4 just above the burning pellet.

Temperature profiles along the laser beam corresponding to the numbered photographs in Figure 4 are presented in Figure 5. One profile corresponds to the moving average of 10 single measurements resulting in a time resolution of 3.3 seconds. A flat, although noisy, temperature profile is observed in the first stage (graph 1) before the pellet has been inserted. Subsequent stages 2, 3 and 4 all show a decrease in temperature above the pellet most likely due to the release of volatile gases in the combustion process. When the visible flames is about to be extinguished in stage 5 a slight increase in temperature is observed and in the final stage a lower temperature above the pellet is observed. The temperature variation along the laser beam demonstrates the need for spatially resolved temperature measurements in these types of situations to fully capture the combustion process and the temperature gradients.

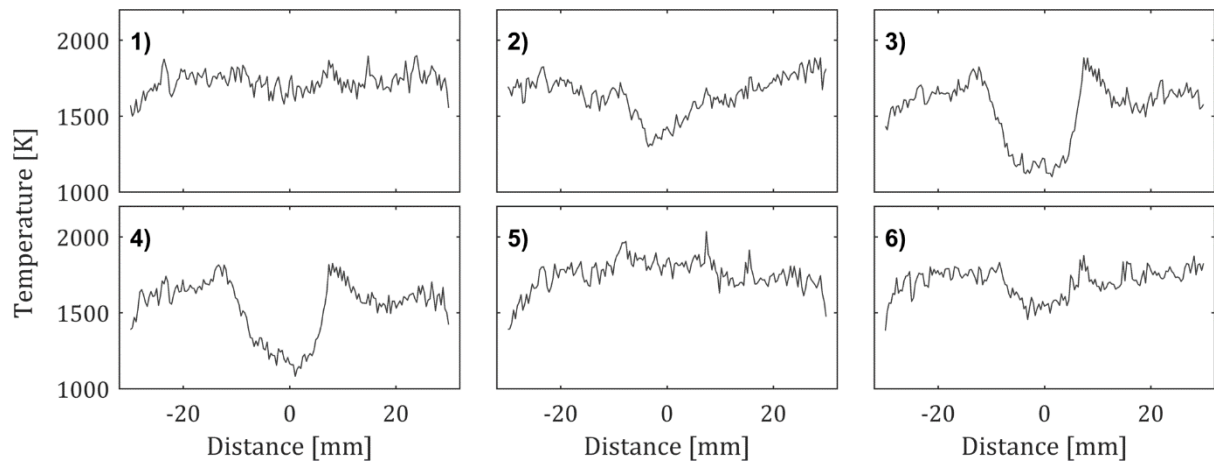


**Figure 5** Radial temperature profiles corresponding to the photographs presented in Figure 4. During the burning of the pellet, frames 3 and 4, a significant decrease in temperature is observed just above the pellet and a secondary reaction zone is observed next to the dip. After the pellet has finished burning, frame 6, the temperature is seen to be lower above the pellet most probably due to heat losses through the ceramic rods.

The time-dependent temperature above the centre of a pellet for the complete combustion process is presented in Figure 6. In the upper panel the temperature of five different pellets are presented and a good agreement between the different pellets are seen both in regards to absolute temperatures as well as in the temporal progression. The mean temperature of the five measurements is shown in the lower panel of Figure 6 with the standard deviation shaded grey. At the start of the measurement the measured temperature is that of the product gas of the flame. When the pellet is inserted into the hot gas environment it heats up and pyrolysis of the pellet occurs. During the pyrolysis stage volatile gas, mainly consisting of species such as CO, CO<sub>2</sub>, H<sub>2</sub>O, H<sub>2</sub>, and CH<sub>4</sub> [8], is released from the pellet, and forms a diffusion flame with oxygen in the hot product gas as shown in Figure 4. The temperature of the volatile gas is shown to be 500 K lower than the temperature of the surrounding product gas. When the release of the volatile gas has finished around 80 s the temperature increases to the surrounding temperature. Char oxidation starts after ~100 s and the temperature above the pellet is somewhat lower than the surrounding gas temperature. This difference may be attributed to heat losses through the ceramic rods as well as perturbations in the gas flow due to the presence of the pellet.

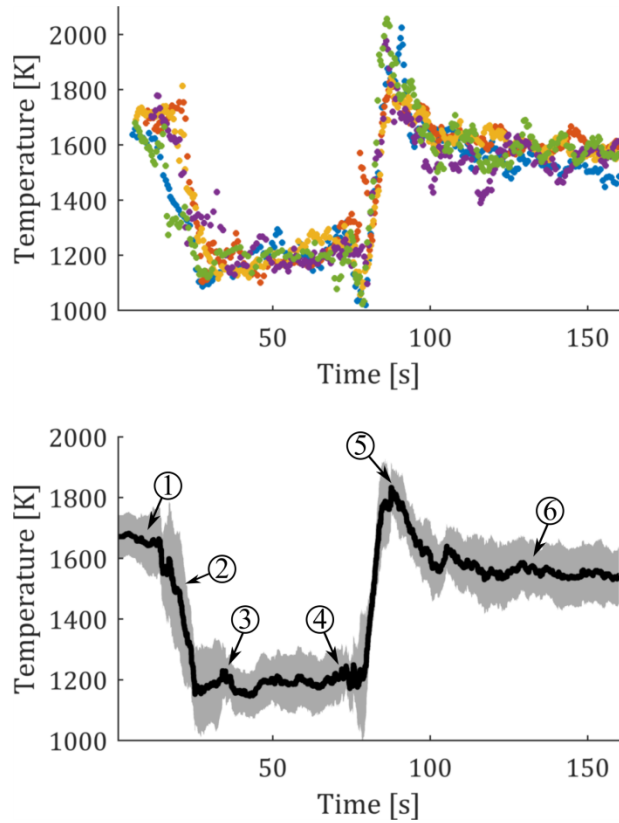


**Figure 6** Upper figure – The temperature above a pellet as a function of time for five different pellet measurements. Good agreement between the five pellets is observed. Lower figure – The average temperature of the five measurements in black and the standard deviation shaded grey. The numbers correspond to the photographs in Figure 4.

The errors related to the accuracy of these types of diode laser-based TLAF measurements have previously been discussed in [18]. There are mainly two sources of error affecting the accuracy significantly: *i*) the laser line-overlap in regards to the absorption line and *ii*) the accuracy of the laser power measurement. The two main sources of error regarding the overlap function are wavelength drifts of the laser during the measurement and a temperature-dependent pressure-shift. The error of each source is  $\sim 2\%$  at flame temperatures. The temperature error from the laser power measurement is liberally estimated to be  $\sim 1.5\%$ , resulting in a total accuracy within  $2.7\%$  at all flame temperatures. To improve the accuracy a frequency locking scheme could be implemented as well as better quantification of the laser powers. The errors of the temperature-dependent pressure shift could also be somewhat mitigated if the pressure shift at different temperatures were better known, although, never fully compensated as the pressure shift is dependent on the gas composition. The precision for the current experiments suffers from low SNR due to the limited dynamic range of the camera. The precision, evaluated as the standard deviation in a region where the temperature is expected to be flat, amounts to  $5\%$  in the product gases of the flame and to  $9\%$  in the region just above the pellet.

## Conclusions

Temperature measurements using diode-laser based two-line atomic fluorescence is demonstrated in a heavily sooting environment such as that from the combustion of wood pellets. A good repeatability is shown for spatially and temporally resolved temperature measurements above burning pellets and it is revealed that the temperature decreases above the burning wood pellet compared to the surrounding gas during the release of volatile gases. These volatile gases form a diffusion flame with the surrounding oxygen. The temperature gradients along the laser beam show the need for spatially

resolved measurements to properly visualize the combustion process. The calibration free thermometric technique is estimated to have an accuracy of  $\sim 2.7\%$ . The precision can be increased dramatically by optimising the measurement conditions, e.g. if only the temperature above the pellet is of interest the signal level can be increased either through a higher seeding concentration or higher camera gain. Extending the spatial measurements to two dimensions through sheet-forming optics should not reduce either accuracy or precision of the technique and will allow for systematic studies of biomass combustion in single-pellet reactors.

### ***Acknowledgements***

The work was financially supported by the Swedish Energy Agency, the Knut & Alice Wallenberg foundation, the Swedish Research Council (VR), the European Research Council (Advanced Grant TUCLA program) and the Danish Council for Strategic Research (the GREEN project).

- [1] L. Gustavsson, P. Börjesson, B. Johansson, and P. Svenningsson, "Reducing CO<sub>2</sub> emissions by substituting biomass for fossil fuels," *Energy*, vol. 20, pp. 1097-1113, 1995/01/01/ 1995.
- [2] D. E. Brune, T. J. Lundquist, and J. R. Benemann, "Microalgal Biomass for Greenhouse Gas Reductions: Potential for Replacement of Fossil Fuels and Animal Feeds," *Journal of Environmental Engineering*, vol. 135, pp. 1136-1144, 2009/11/01 2009.
- [3] P. Basu, J. Butler, and M. A. Leon, "Biomass co-firing options on the emission reduction and electricity generation costs in coal-fired power plants," *Renewable Energy*, vol. 36, pp. 282-288, 2011/01/01/ 2011.
- [4] M. Mann and P. Spath, "A life cycle assessment of biomass cofiring in a coal-fired power plant," *Clean Products and Processes*, vol. 3, pp. 81-91, 2001/08/01 2001.
- [5] M. E. Goerndt, F. X. Aguilar, and K. Skog, "Drivers of biomass co-firing in U.S. coal-fired power plants," *Biomass and Bioenergy*, vol. 58, pp. 158-167, 2013/11/01/ 2013.
- [6] L. J. R. Nunes, J. C. O. Matias, and J. P. S. Catalão, "Mixed biomass pellets for thermal energy production: A review of combustion models," *Applied Energy*, vol. 127, pp. 135-140, 2014/08/15/ 2014.
- [7] T. Miranda, I. Montero, F. J. Sepúlveda, J. I. Arranz, C. V. Rojas, and S. Nogales, "A Review of Pellets from Different Sources," *Materials*, vol. 8, pp. 1413-1427, 2015.
- [8] H. Fatehi and X. S. Bai, "A Comprehensive Mathematical Model for Biomass Combustion," *Combustion Science and Technology*, vol. 186, pp. 574-593, 2014/05/04 2014.
- [9] H. Fatehi, Z. Qu, F. M. Schmidt, and X.-S. Bai, "Effect of Volatile Reactions on the Thermochemical Conversion of Biomass Particles," *Energy Procedia*, vol. 105, pp. 4648-4654, 2017.
- [10] A. A. Bhuiyan and J. Naser, "CFD modelling of co-firing of biomass with coal under oxy-fuel combustion in a large scale power plant," *Fuel*, vol. 159, pp. 150-168, 2015/11/01/ 2015.
- [11] J. M. Jones, M. Pourkashanian, and A. Williams, "Biomass combustion modelling," *International Journal of Ambient Energy*, vol. 21, pp. 115-123, 2000/07/01 2000.
- [12] P. E. A. Debiagi, G. Gentile, M. Pelucchi, A. Frassoldati, A. Cuoci, T. Faravelli, *et al.*, "Detailed kinetic mechanism of gas-phase reactions of volatiles released from biomass pyrolysis," *Biomass and Bioenergy*, vol. 93, pp. 60-71, 2016/10/01/ 2016.
- [13] W. Weng, Q. Gao, Z. Wang, R. Whiddon, Y. He, Z. Li, *et al.*, "Quantitative measurement of atomic potassium in plumes over burning solid fuels using infrared-diode laser spectroscopy," *Energy & Fuels*, vol. 31, pp. 2831-2837, 2017.
- [14] Z. Qu and F. M. Schmidt, "In situ H<sub>2</sub>O and temperature detection close to burning biomass pellets using calibration-free wavelength modulation spectroscopy," *Applied Physics B*, vol. 119, pp. 45-53, 2015/04/01 2015.
- [15] J. Engström, J. Nygren, M. Aldén, and C. F. Kaminski, "Two-line atomic fluorescence as a temperature probe for highly sooting flames," *Opt. Lett.*, vol. 25, pp. 1469-1471, 2000.
- [16] J. E. Dec and J. O. Keller, "High speed thermometry using two-line atomic fluorescence," *Symposium (International) on Combustion*, vol. 21, pp. 1737-1745, 1988.
- [17] C. T. J. Alkemade, "A theoretical discussion on some aspects of atomic fluorescence spectroscopy in flames," in *Pure and Applied Chemistry* vol. 23, ed, 1970, p. 73.
- [18] J. Borggren, W. Weng, A. Hosseinnia, P. E. Bengtsson, M. Aldén, and Z. S. Li, "Diode laser based thermometry using two-line atomic fluorescence of indium and gallium," *Submitted to Applied Physics B*, 2017.
- [19] A. C. Eckbreth, *Laser diagnostics for combustion temperature and species* vol. 3: CRC Press, 1996.
- [20] I. S. Burns, X. Mercier, M. Wartel, R. S. M. Chrystie, J. Hult, and C. F. Kaminski, "A method for performing high accuracy temperature measurements in low-pressure sooting flames using two-line atomic fluorescence," *Proceedings of the Combustion Institute*, vol. 33, pp. 799-806, 2011.

- [21] J. Hult, I. S. Burns, and C. F. Kaminski, "Two-line atomic fluorescence flame thermometry using diode lasers," *Proceedings of the Combustion Institute*, vol. 30, pp. 1535-1543, 2005.
- [22] R. S. M. Chrystie, I. S. Burns, J. Hult, and C. F. Kaminski, "High-repetition-rate combustion thermometry with two-line atomic fluorescence excited by diode lasers," *Opt. Lett.*, vol. 34, pp. 2492-2494, 2009.
- [23] H. Haraguchi, B. Smith, S. Weeks, D. J. Johnson, and J. D. Winefordner, "Measurement of Small Volume Flame Temperatures by the Two-line Atomic Fluorescence Method," *Appl. Spectrosc.*, vol. 31, pp. 156-163, 1977.
- [24] R. Whiddon, B. Zhou, J. Borggren, M. Aldén, and Z. Li, "Vapor phase tri-methyl-indium seeding system suitable for high temperature spectroscopy and thermometry," *Review of Scientific Instruments*, vol. 86, p. 093107, 2015.
- [25] O. M. Maragò, B. Fazio, P. G. Gucciardi, and E. Arimondo, "Atomic gallium laser spectroscopy with violet/blue diode lasers," *Applied Physics B*, vol. 77, pp. 809-815, 2003// 2003.
- [26] W. Weng, J. Borggren, B. Li, M. Aldén, and Z. Li, "A novel multi-jet burner for hot flue gases of wide range of temperatures and compositions for optical diagnostics of solid fuels gasification/combustion," *Review of Scientific Instruments*, vol. 88, p. 045104, 2017.
- [27] Q. N. Chan, P. R. Medwell, P. A. M. Kalt, Z. T. Alwahabi, B. B. Dally, and G. J. Nathan, "Solvent effects on two-line atomic fluorescence of indium," *Applied Optics*, vol. 49, pp. 1257-1266, 2010/03/10 2010.